Investigation of plasma characteristics of center region of post cylindrical magnetron sputtering device

Baha T. Chied, Rahman R .Abdula, Qusay A. Abbas

Department of Physics, College of Science, University of Baghdad, Jadiriya, Baghdad, Iraq

Abstract

A d.c. magnetron sputtering system was designed and fabricated. The chamber of this system is consisted from two copper coaxial cylinders. The inner one used as the cathode and the outer one used as anode with magnetic coil located on the outer cylinder (anode). The axial behavior of the magnetic field strength along the cathode surface for various coil current (from 2A to 14A) are shown. The results of this work are investigated by three cylindrical Langmuir probes that have different diameters that are 2.2mm, 1mm, and 0.45mm. The results of these probes show that, there are two Maxwellian electron groups appear in the central region. As well as, the density of electron and ion decreases with increases of magnetic field strengths.

Keywords

cylindrical magnetron sputtering plasma characteristics.

Article info

Received: Aug.

Accepted: Fab.

Published: Dec.

دراسة خصائص البلازما في منطقة المركز لمنظومة الترذيذ الماكنترون ذات الأبعاد الأسطوانية

بهاء طعمة جياد , رحمن رستم عبد الله , قصي عدنان عباس

جامعة بغداد – كلية علوم – قسم الفيزياء

الخلاصة:

في هذا العمل تم تصميم و تكوين منظومة الترذيذ الماكنترون. ان حجرة هذا المنظومة تتكون من اسطوانتين نحاسيتين ذات محور مشترك. حيث استخدمت الاسطوانة الداخلية كقطب سالب اما الاسطوانة الخارجية استخدمت كقطب موجب حيث يكون الملف المغناطيسي موضوع على السطح الخارجي للاسطوانة الخارجية (الانود). تم دراسة توزيع المجال المغناطيسي المتولد في الملف لتيارات مختلفة تتراوح بين (2 إلى 12 أمبير). ان نتائج هذا العمل قد فحصت باستخدام ثلاثة مجاميع من مجسات الانجمور الأسطوانية مختلفة الأقطار وهي 1 ملي متر,ملي متر 0.45,ملي متر 2.2 . أن نتائج هذه المجسات قد بينت بان هناك مجموعتين من الإلكترونات مختلفة الطاقة تخضع لتوزيع ماكسويل تظهر في منطقة المركز. بالإضافة إلى ذلك فقد لوحظ بان كثافة الإلكترون و الأيون تقل مع زيادة قوة المجال المغناطيسي.

Introduction

Sputtering entails the bombardment of a target with energetic particles (usually positive gas ions) which cause some surface atoms to be ejected from the target. These ejected atoms deposit onto any solid that may be close to the target. This phenomenon has been known for well over a century, and sputtering was used as a method for depositing a film as early as 1877 [1].

Magnetron sputtering uses magnetic field transverse to the electric field at sputtering target surface. This external magnetic field parallel to the cathode (target) will cause target traps of energetic electrons in their travel from the cathode to the anode leading to an amplification of gas ionization. Also, the magnetic field will increase the path length of the electrons before the anode collects them, and keeping electrons away from the vacuum chamber, and ensures a sufficiently high ionization rate [2,3]. There are several types of magnetron for practical application. The most common configurations are; planner, cylindrical, and circular [4].in cylindrical magnetron configuration the electrodes of magnetron has a cylindrical geometry and an axial magnetic field, with the inner one used as the target. This arrangement is knows as a cylindrical magnetron or post magnetron. This configuration has the ability to coat a large area of small substrate [3,4]. When the inner cylinder is anode, the arrangement is known as an inverted magnetron.

In the cylindrical magnetron system, there are two different modes of glow discharge appear. One is a positive space charge dominated mode (PSC mode) which appears with a weak magnetic field. The other is a negative space charge dominated mode (NSC mode) which appears with a strong magnetic field [5]

In all types of magnetrons a specific configuration of an external magnetic field is applied to trap electrons in a region close to cathode, this allows the magnetron to operate at lower pressures and voltage than within the other devices [6].

Experimental Set Up

A d.c. cylindrical magnetron sputtering is designed and fabricated. This system is consisting of two coaxial copper cylinders the inner one used as a cathode and the outer one used as anode. The diameters of the inner and outer cylinder are 1.9 cm and 9.8 cm, respectively and 22cm length. This system can be seeing in figure (1).

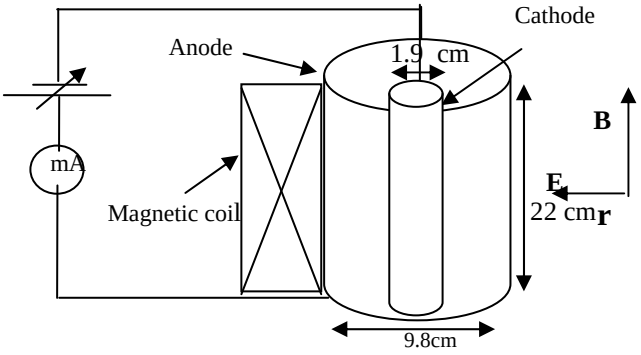

Figure (1): Schematics of cylindrical magnetron device.

The working principle of this device is the glow discharge between the electrodes. In this device, the normal glow discharge is produced when a dc. constant voltage of about 2.4kV is applied between the two coaxial cylindrical electrodes. Due to this external voltage, the argon plasma discharge is formed and then the electrodes voltage will drop. The dc. magnetic field (that is generated by passing the dc. current in the solenoid coil) is superposed transversely onto the electric field direction (see figure (1)). Figure (2) estimated the magnetic field profile along the cathode surface as a function of the coil currents.

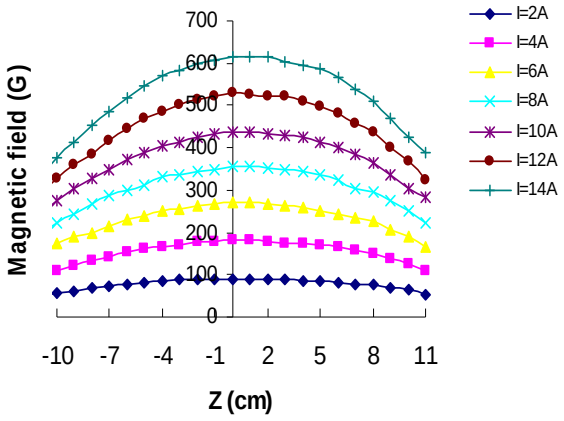

Figure (2): The magnetic field profile for various

Results and Discussion

According to our magnetic field configuration, the central region of the magnetron represents a good trap region for electrons that are used to maintain the glow discharge because of the presence of strong electric and magnetic fields. The coordinates of this region occurs at Z= 0cm (where Z=0 refers to 11cm height from the bottom of cylinders).

Three groups of cylindrical Langmuir probes of 2.2mm, 1mm, and 0.45mm diameters are used to determine the plasma characteristics in this region. The first and the second groups consist of a tungsten wire of 2.2mm and 1mm in diameter, respectively, which are covered by a thin ceramic tubes with outer diameter of 9mm to insulate it from the plasma expect for a short length of exposed tip. While in the third group, a tungsten wire 0.45mm in diameter is threaded into a glass tube with outer diameter of 5mm to insulate it from the plasma. The length of the exposed tip is 4mm that is used in all cylindrical probes that are designed. The probe tip is located in the center of the insulator tubes and is extended out of its end without touching it.

According to the experimental data of these probes, Figures (3) and (4) illustrates the effect of the magnetic field strength on the electron and ion saturation currents, respectively, at different radial positions. It is clear from figures (3) and (4) that the electron and ion saturation currents decrease with the increase of the magnetic field strength in both radial positions. These decreases in both saturation currents could be attributed to the electrons and ions collisions with neutral argon atoms.

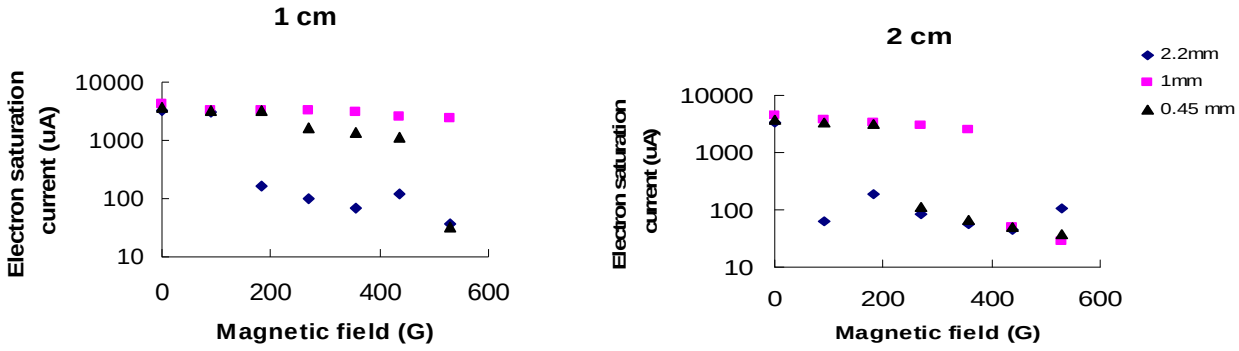

Figure (3): Electron saturation currents versus magnetic field for different probe diameter at different radial positions at pressure 4x10^{-4}mbar.

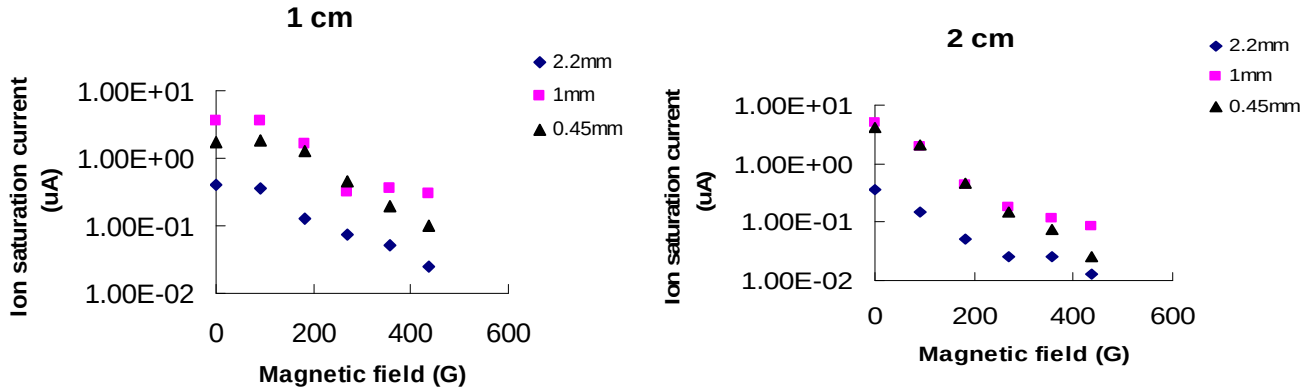

Figure (4): Ion saturation current versus magnetic field for different probe diameter at different radial position.

In addition to the above measurements, the floating potential (V_f) is calculated (It is the potential at which no net current is drawn). The variation of this potential with magnetic field strength at different radial positions is plotted in figure (5). It is explicit from this figure that the floating potential increases negatively with increasing of the magnetic field strength. Such behavior may be associated with the existence of high-energy electron flux.

These electrons that are approaching the probe are both larger and more energetic than in any other direction. Therefore, the probe becomes more negative before electron and ion currents are equalized. The important feature of this result is that, the floating potential (calculated for different probe diameter) goes to positive values as the distance from the cathode surface increases. This result caused by the magnetic field will confine the electron near the cathode reducing its motion towards the anode.

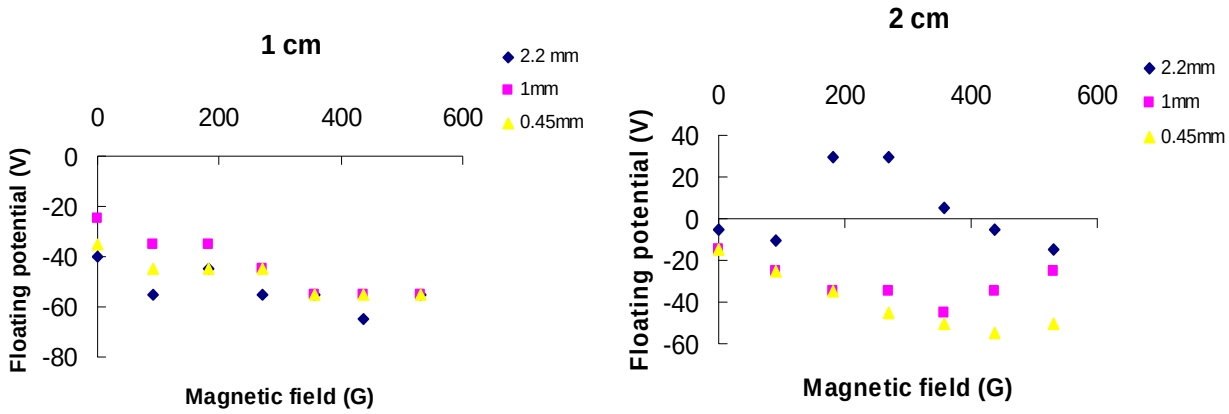

Figure (5): Effect of magnetic field on the floating potential at different radial positions for different probe diameters at pressure of $4x10^{-4}$ mbar.

From the experimental data of I-V curve of Langmuir probes which have different diameters (which not shown here) we found the straight line of the transition region is broken into two straight lines. This fact verified that, there are two distinct Maxwellian distribution of electrons with different energies, cold and hot electrons with temperatures T_{ec} and T_{he}, respectively. The slopes of these two straight segments would give the temperatures of the two groups. Figures (9) and (10) show the hot and cold electron temperatures as a function of magnetic field that is measured by 2.2mm, 1mm, and 0.45mm diameter probes at the central region for different radial positions from the cathode surface.

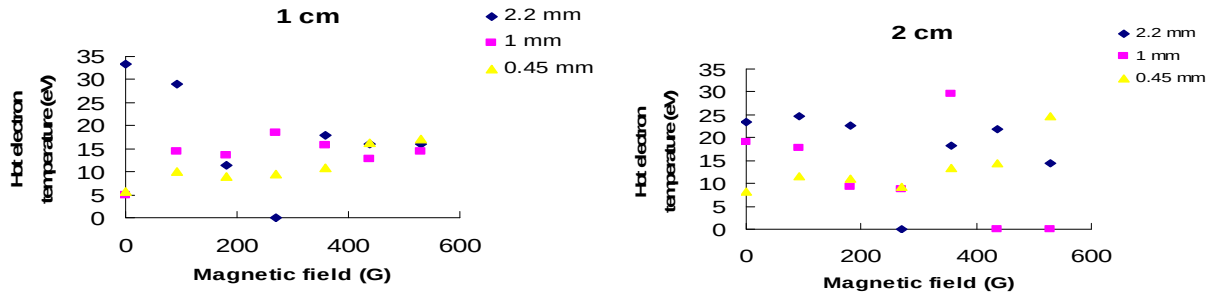

Figure (6): Typical hot electron temperatures against the effect of magnetic field as detected by 2.2 mm, 1mm, and 0.45 mm diameters probes.

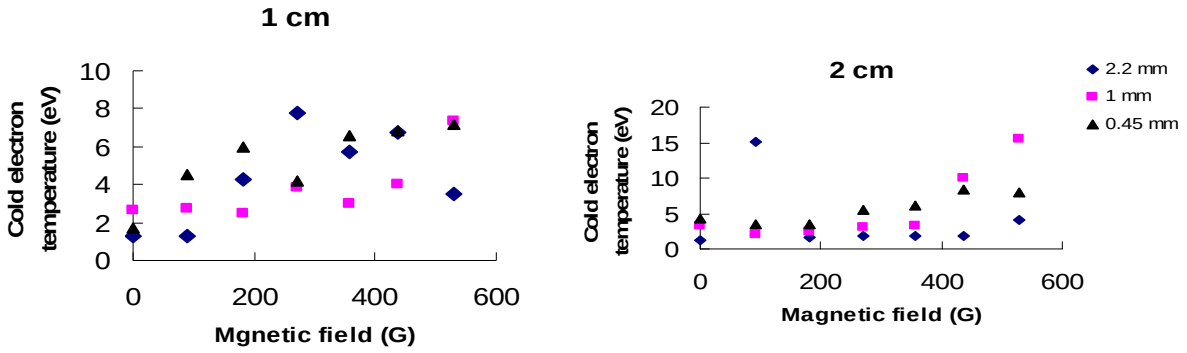

Figure (7): Typical cold electron temperatures against the effect of magnetic field as detected by 2.2 mm, 1mm, and 0.45 mm diameters probes.

Comparing the curves of figure (6) illustrates that, at a radial position of 1cm, the hot electron temperature increases with increasing of the magnetic field as measured by the 1mm and the 0.45mm diameters probes. While using the 2.2mm diameter probe, the hot electron temperature decreases slightly as the magnetic field strength increases reaching zero when the magnetic field about 270G (corresponding to I_{coil}= 6A) before it starts to increase with increasing of the magnetic field strength. These differences in measurements among the probes may be caused by the contamination of the probe tip (where the contamination of the probe increasing with increasing the probe radius [7, 8]). At a radial position 2cm, the hot electron temperature decreases to a minimum value at a magnetic field strength of about 270G before it starts to increase again with increasing the magnetic field strength. This behavior is noted for all probe diameters. Furthermore, the decrease of the hot electron temperature with increasing the magnetic field strength can be due to the collisions with the neutral argon atoms. This happens for magnetic field strength less than 270G. Above 270G, the electron gyro radius will decrease further and the electron collision probability will decrease so the electron temperature increases.

The experimental data of cold electron temperature (which is plotted in figure (7)) shown that the increase of cold electron temperature with the increase of the magnetic field strength at distance 1cm. While at radial position 2cm, the cold electron temperature is approximately independent on the magnetic field strength before starts slightly to increase in magnetic field up 357G.

The plasma potential (that obtained by drawing a straight line through the I-V curve in the transition and the electron saturation current regions) as a function of magnetic field are plotted in figure (8). These data illustrate that, as indicated from 2.2mm diameter probe, the plasma potential has positive values and it decreases with increasing of the magnetic field strength at both radial positions. On the other hand, according to 1mm diameter probe, the plasma potential shows a slightly increase with increasing the magnetic field strength at both radial positions.

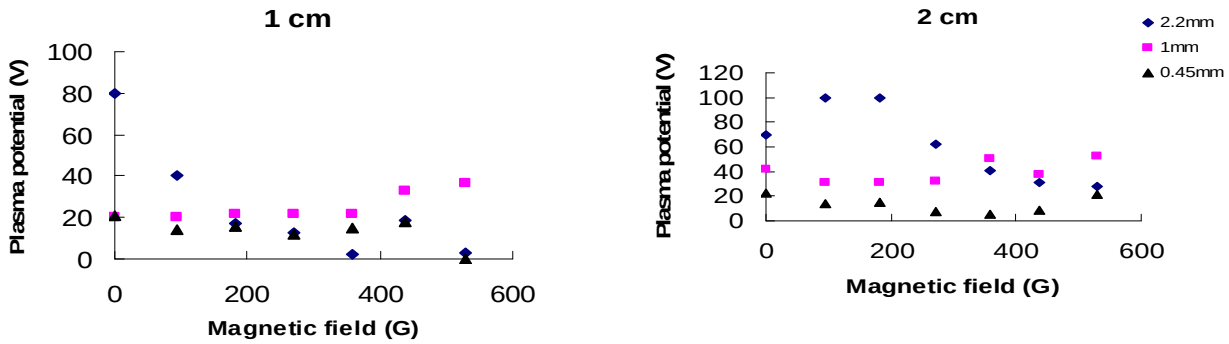

Figure (11): The variation of plasma potential with magnetic field at ***different radial positions for different probe diameters.***

However, the cold and hot electron densities are calculated from [9]:

$$n_e = 4I_{es} / e v_{e,th} A_{probe} \qquad (1)$$

where e, I_{es}, A_{probe}, and $v_{e,th}=\sqrt{8kT_e/\pi m_e}$ are electronic charge, electron saturation current, probe area, and the average electron thermal speed, respectively. If the electron saturation current (taken from figure (3)) and the hot and cold electron temperatures (taken from figures (9) and (10)) are substituted into equation (1), the variation of the cold and hot electron density densities with the magnetic field at both radial positions for different probe diameters will be obtained as plotted in figures (12) and (13), respectively. The comparison of both figures shows that the density of the cold electron is greater than the hot electron density in both radial positions. Furthermore, the hot and cold electron densities decrease with increasing of the magnetic field strength. According to experimental data of 2.2mm probe diameter found that the hot electron density reduces to zero in both radial positions at magnetic field strength equal to 270G. While, for 1mm diameter probes, the hot electron density reduces to zero for magnetic field strength greater than 458G. These results indicate that the 2.2mm diameter probe detects only one group of electrons when the magnetic field strength is equal to 270G for both radial positions. While, for 1mm diameter probes, one group of electrons is detects at radial a position 2cm for the magnetic field strength above 358G.

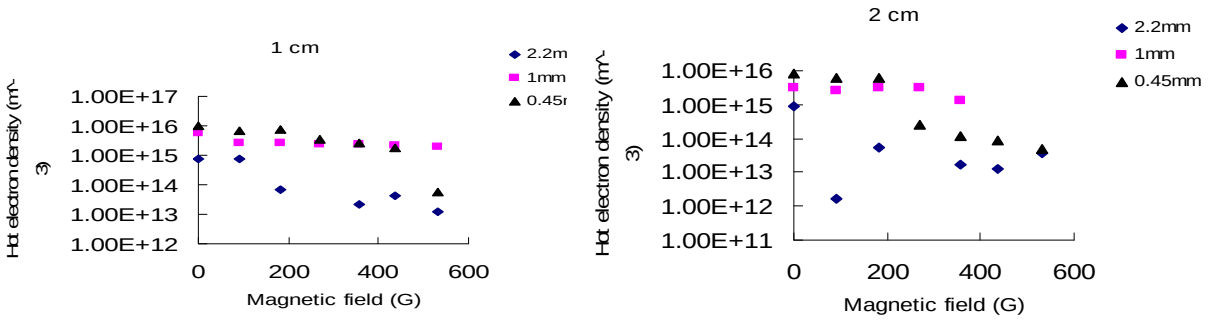

Figure (12): The variation of the hot electron densities versus magnetic field strength for different probe diameters at different radial positions.

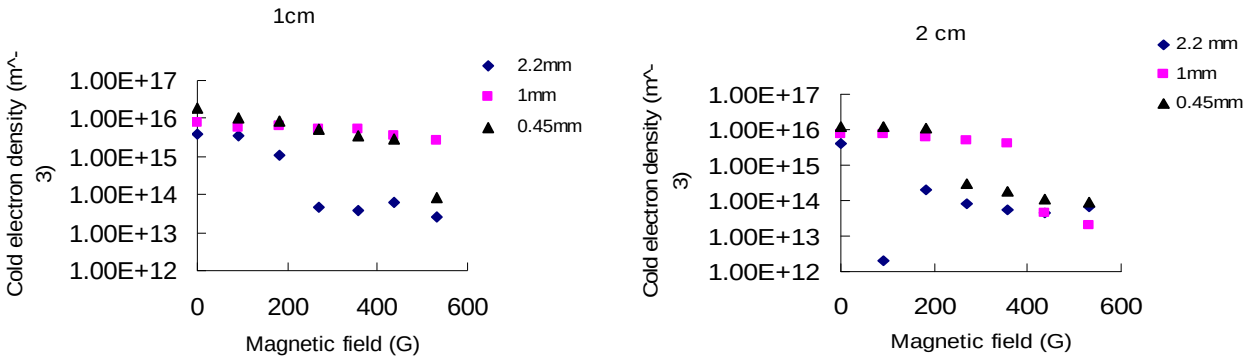

Figure (13): The variation of the cold electron densities versus magnetic field strength for different probe diameters at different radial positions.

Since there are two electron groups with different energies, then, the electron probe current is written as [9]:

$$I_e(V) = I_{ec}(V) + I_{eh}(V) \qquad (2)$$

I_{ec} and I_{eh} represent the cold and hot electron currents, respectively. So that, the electron density in this case is evaluated as:

$$n_e = n_{ec} + n_{eh} \qquad (3)$$

Considering the values of n_{ec} and n_{eh} from figures (12) and (13), the results of the equation (3) are plotted in figure (14). The results of this figure show that, at both radial positions, the electron density decreases with the increase of the magnetic field strength.

The decrease of electron density with increasing of magnetic field strength is caused by the electron temperature that increases with the magnetic field strength as well as the losses of electron that attributed to the magnetic field strength.

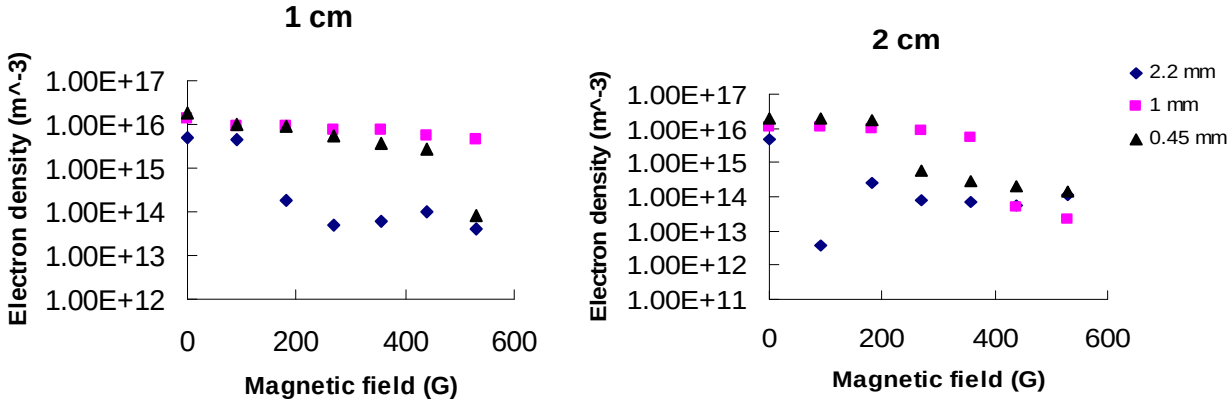

Figure (14): The variation of electron density with magnetic field at different radial positions for different probe diameters.

The electron temperature in the case of apparent of two groups with different energy, can estimated as [9]:

$$\frac{1}{T_e} = \left(\frac{n_{ec}}{n_e}\right)\frac{1}{T_{ec}} + \left(\frac{n_{eh}}{n_e}\right)\frac{1}{T_{eh}} \qquad (4)$$

Considering the values of n_{eh} and n_{ec} from figures (12) and (13), and T_{he} and T_{ec} from figures (9) and (10), the result of equation (4) is plotted in figure (15).

the cold electron temperature with increases of the magnetic field strength. This behavior are caused by the cold electron density are greater than from the hot electron density.

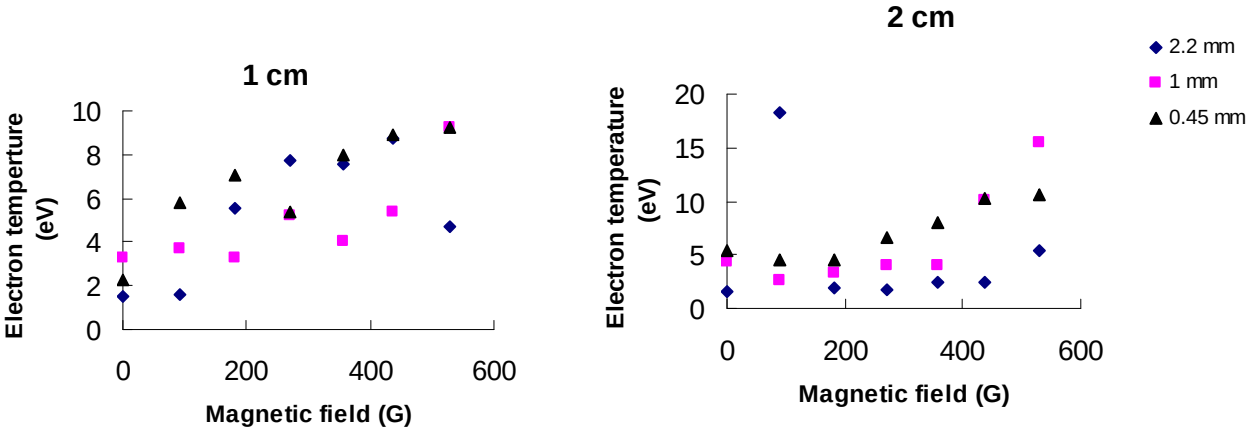

Figure (15): the effect of magnetic field strength on the electron temperature for different radial positions and different probe diameters.

References

[1] R. Berry, P. Hall, and M. Harris, "Thin Film Technology", VAN Nostrand Reinhold Company, New York,(**1968**).

[2] K. Hinkel, "Magnetrons", Cleaver-Hume Press Ltd., London, 1961.

[3] J. Vossen, "Thin Film Processes", Academic Press, INC., New York, (**1978**).

[4] B.Chapman, "Glow Discharge Processes ", John Wiely & Sons, INC, New York, (**1980**).

[5] K. Wasa, and S. Hayakawa, "Low pressure sputtering system of the magnetron type, "The Review of Scientific Instruments", 40, 5, 693, (**1969**).

[6] T. Sheridan, M. Goeckner, and J. Goree, Observation of two-temperature electrtons in a sputtering magnetron plasma, "J.Vac. Technol.", A9, 3, 688, (**1991**).

[7] P. Chung, L. Talbot, and K. Touryan, "Electric Probes in Stationary And Flowing Plasmas: Theory and Application", Soringer-Verlag, Berlin-Heidelbery, New York, (**1975**).

[8] R. Huddleston, and S. Leonard," Plasma Diagnostic Techniques", Academic Press, Inc., New York, **1965**.

[9] R. Merlino," Understanding Langmuir probecurrent-voltage characteristics", American J. Phys., 75, 12, 1078, (**2007**).